doi:10.2533/chimia.2026.120 Chimia 80 (2026) 120–124

Nanopore Studies of DNA Damage and G-quadruplex Folding in the Human Telomere Sequence

Aaron M. Fleming* and Cynthia J. Burrows*

Abstract: The bacterial pore-forming toxin α-hemolysin has dimensions appropriate for capture and translocation of DNA strands in a single-molecule electrophoresis experiment. We used the nanopore's properties to study G-quadruplex unfolding in the human telomere repeat sequence with and without the presence of DNA lesions introduced into either the GGG tracks of a potential G-quadruplex (*via* oxidation) or the TTA loops (*via* photodimerization). Different topological folds of the G-quadruplex could be distinguished by either their current-time signatures or by their unfolding rates when a dA_{25} tail was added. Another more compact four-stranded structure, the i-motif, was also studied and found to be exceptionally well folded and stable inside the nanopore cavity. Comparisons are made between early studies with a home-built nanopore device *vs*. the currently available instrument from Oxford Nanopore Technologies (ONT), showing that we approach, but do not yet achieve, single-molecule sequencing of DNA damage sites in human telomere repeats. These studies aid in our understanding of the structure and dynamics of non-canonically folded DNA, its behaviour in crowded environments that mimic intracellular conditions, and the ability to use nanopore sequencing to identify DNA damage sites in this oxidation-prone segment of the genome.

Keywords: DNA damage · G-quadruplex · i-Motif · Nanopore · Telomere

From left to right: Aaron Fleming, Cynthia Burrows

Aaron M. Fleming is currently a research associate professor in chemistry at the University of Utah, and he will begin an independent tenure-line position there on July 1st 2026. He has broad expertise in nucleic acid chemistry and specifically in both G-quadruplex DNA analysis and in the use of nanopore sequencing technology for DNA and RNA modification detection.

Cynthia J. Burrows is a distinguished professor and holds the Thatcher Chair in biological chemistry at the University of Utah. Her research program focuses on defining the chemistry and biological outcomes of oxidative stress in DNA and RNA. As part of this program she has developed nanopore sequencing tools to investigate DNA damage in G-rich sequences such as telomeres and gene promoters, where G-quadruplex structures both are a target of damage and play key roles in the response to oxidation. Some of this work was presented at the EFMC-ISCB 2025 in Basel, CH.

1. Nanopore Basics

An emphasis on personalized medicine helped launch the $1000 Genome Project in 2004 with the idea that easy access to an individual's complete genetic code would permit medical treatment targeted to specific disease origins. In collaboration with Henry White at the University of Utah, we joined the race to find low-cost, single-molecule approaches to the analysis of a DNA sequence and structure through the study of protein nanopores interacting with DNA in an electrophoretic device.[1] By 2010, several research groups had homed in on α-hemolysin (α-HL), a bacterial protein that self assembles into a homoheptamer with a β-barrel domain inserted into a lipid bilayer and a vestibule at one end of a central pore (Fig. 1).[2] When a potential of 120 mV is applied across the bilayer, polyanionic DNA (or RNA) strands are captured in the vestibule, and unfolded single strands can translocate through the central pore. Monitoring electrical current *vs.* time (*i-t*) provides information about the nucleic acid occupying the pore, and in particular, the number of ions/μs that can flow through the 1.4-nm constriction reflects the structure and solvation state of oligonucleotides.[3]

While biotech companies were spending billions to create robust sequencing platforms based on nanopore technology, our labs, with three orders of magnitude less funding, focused on the basic science we could learn from interactions of protein nanopores with DNA containing either alternative folding patterns or alternative bases, or both. Here, we focus on studies of the human telomere (hTelo) repeat sequence, $d(GGGTTA)_n$, because it is both capable of folding to G-quadruplex (G4) structures and is a site highly susceptible to oxidative damage.[4,5] Our studies from 2008 to 2020 used a device designed by the White laboratory in which a single α-HL heptamer was embedded in a lipid bilayer

*Correspondence: Prof. C. J. Burrows, E-mail: burrows@chem.utah.edu; Prof. A. M. Fleming, E-mail: afleming@chem.utah.edu
Department of Chemistry, University of Utah, Salt Lake City, UT 84112-0850, United States

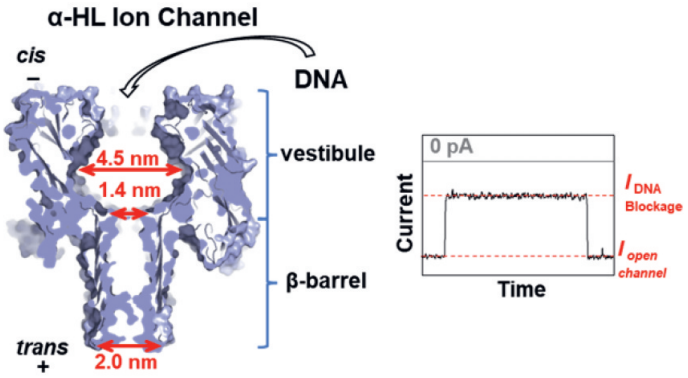

Fig. 1. The α-hemolysin nanopore has dimensions that permit monitoring of ionic current changes while DNA translocates through the channel.

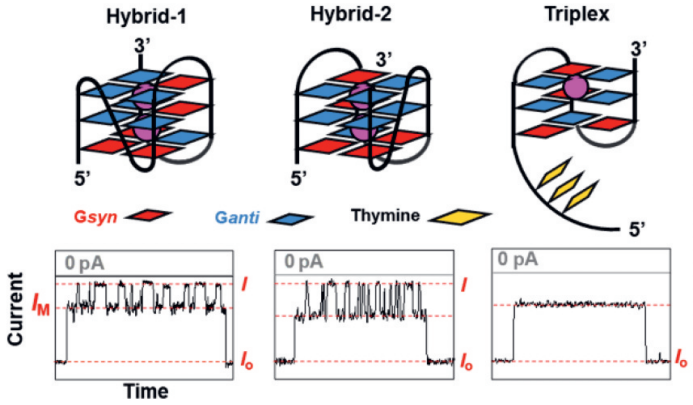

Fig. 2. The hTelo hybrid-1 and hybrid-2 G4 folds and the triplex structure yield diagnostic ionic current patterns for the different topologies.

spanning a 1-μm opening in a glass membrane.[1,6] Current measurements showed accuracy in the pA range with ~μs time resolution, and these parameters were appropriate for monitoring the capture and translocation of single molecules of DNA, typically of lengths 40–200 nucleotides.

2. Nanopore Studies of G-Quadruplex Folds

G-quadruplexes (G4s) can be formed in strands of DNA containing, typically, four sets of 5'-GGG-3' sequences.[7] One G from each set comes together in a Hoogsteen hydrogen-bonded array forming a tetrad, and 3 tetrads stack to provide a stably folded G4 motif. The monovalent cations Na^+ or K^+ occupy central positions between tetrads, leading to slightly different orientations of the GGG runs; in the presence of Na^+, the G tracks are often antiparallel with TTA loops, whereas in high salt concentrations (>1 M), the oligonucleotide is dehydrated and forms a parallel-stranded G4.[8,9] In physiological salt, 140 mM K^+, hybrid folds have been determined for the telomere sequence (hTelo) that involve a 3+1 mixture of strand orientations. This led to our first nanopore challenge.

G-Quadruplexes are of considerable current interest because they occur in gene regulatory regions of mammalian genomes; for example, in promoters they serve as transcription factor hubs, often resulting in upregulation of the gene.[10] Because many of these genes are cancer associated, G4 sequences are of great interest as potential drug targets.[7] G4s also occur in telomere regions that cap the ends of chromosomes; because telomere shortening is of critical importance in both cellular senescence and cancer, the susceptibility of G4s to oxidative DNA damage and strand cleavage is of high interest.[11]

2.1 *Probing G4 Folds with α-HL*

The vestibule of the α-HL heptamer has a volume of about 40 nm^3 and an opening to bulk solvent that is ~3 nm in diameter. This suggested to us that the different folds of the hTelo G4 might interact differently with the α-HL vestibule, resulting in distinct *i-t* signatures. At the time of this first study, 2013, there was controversy about the exact structure of the physiologically relevant hybrid folds because NMR and optical tweezer experiments led to different conclusions about which loop was a double-chain reversal (Fig. 2), the 5' loop leading to the hybrid-1 fold or the 3' loop leading to hybrid-2.[4,7,8] Because the two hybrids have somewhat different sizes and shapes, we hoped to distinguish these by examining single-molecule *i-t* traces while the folded structures were captured in the vestibule.

In the experiment, 5'-TAGGG$(TTAGGG)_3$TT-3', which contains a centrally folded G4 with 2-nt overhanging 3' and 5' ends, could be captured in the α-HL vestibule and held for several seconds before bouncing back out of the pore opening.[12] Oscillations in current between partially blocked (30–40% of open channel current, I_o) and strongly blocked (10% I_o) were attributed to the 2-nt tail being drawn into the constriction channel, but the majority of the G4s did not unfold. After collecting current signatures for >500 molecules, the *i-t* traces could be sorted into 3 types, present in a ratio of 11:5:1 and representing hybrid-1, hybrid-2, and a partially unfolded triplex. These assignments were made possible by synthesizing analogous sequences with known folding properties. For example, the hybrid structures have specific Gs present in the *syn* rather than the normal *anti* glycosidic bond conformation, and these structures could be induced by judicious replacement of G by 8-BrG, a nucleoside that strongly prefers to be *syn*.[13] Similarly, the triplex could be simulated by replacing a GGG track with TTT.[14] Authentic mixtures of folds could then be used to calibrate the findings. In the end, we found that for short hTelo sequences, the hybrid-1 fold is favoured over hybrid-2 by about 2:1.[12]

2.2 *Probing G4 Unfolding with α-HL*

The observation that 2-nt tails on G4s were electrophoretically drawn into the constriction zone of the pore suggested to us that longer single-stranded overhangs might provide the opportunity to study G4 unfolding under an applied force. For this study, we added dA_{25} to the 5' end of the prior hTelo sequence.[9] The poly-dA tail was readily captured by the vestibule when a 120 mV potential was applied across the pore, and it then rapidly threaded into the constricted channel. There, the folded G4 presented a steric block, but when the G4 eventually unfolded under this ~10 pN force, the strand rapidly translocated to the other side of the pore (Fig. 3). For 19% of the single-molecule events, we observed a transient intermediate current level consistent with the partially unfolded triplex structure before final unfolding and translocation.

The hybrid-folded G4 showed high stability under the electrophoretic force applied with unfolding times of ~4 min. In contrast to the kinetic stability of hybrid-folded hTelo G4 in K^+ solution, the antiparallel or 'basket' conformation formed in Na^+ solution was more readily unravelled at the same applied force, and the median lifetime in the pore before unfolding was 2–3 orders of magnitude shorter for the more spherically shaped basket fold (Fig. 3). We attribute these differences to the crowded environment within the vestibule that inhibited the hybrid G4 from rolling in the protein cavity. Even though the basket-folded G4 is thermodynamically more stable (T_m = 72 °C) compared to the hybrid one (T_m = 60 °C), its spherical shape allows it to roll inside the vestibule and therefore unravel under the electrophoretic force applied to the dA_{25} tail.

Many G4 sequences prefer to fold into a parallel G4; however, the hTelo sequence must be coerced into the parallel (aka 'propeller') conformation by use of high salt, dehydrating conditions.[9]

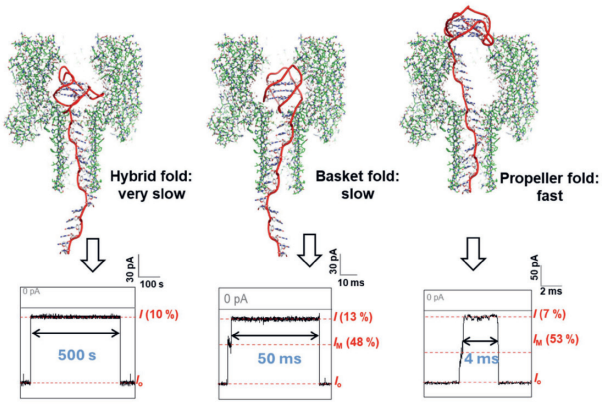

Fig. 3. The hybrid, basket, and propeller folds of the hTelo sequence display fold-dependent unfolding kinetics in the α-HL nanopore.

We prepared this structure in 5 M LiCl with 50 mM KCl present for G4 binding. These conditions give rise to a very viscous solution for which one would expect unfolding rates to be very slow. In contrast, we found that the propeller-folded G4 unfolded 10x faster than the basket fold in the nanopore experiment. We again attribute this outcome to shape — the propeller-folded G4 is disc-like with a diameter of 4.0 nm, too large to enter the 3.0 nm opening to the vestibule. Consequently, threading of the dA_{25} tail into the nanopore leaves the G4 knot outside of the vestibule in bulk solution, leading to rapid and unencumbered unravelling of the G4.[12] RNA G-quadruplexes exist principally in the parallel-folded state, and consequently we do not anticipate that they would not enter the vestibule to give characteristic signatures.

2.3 *Probing i-motif Unfolding with α-HL*

The complementary strand of the hTelo sequence is rich in cytidine: 5'-$(TAACCC)_n$-3', and when n≥4, the strand can fold into an intercalated motif (i-motif) stabilized by hemi-protonated C^+-C base pairs (Fig. 4).[15] The stability of the folded i-motif depends on the pH; for the hTelo sequence, the midpoint transition is pH_T 6.1, *i.e.* the pH at which 50% of the sequence is folded.[16,17] At pH 5.0, the strand is 100% folded into a 4-stranded compact structure with 3 hairpin loops.

The diameter of the folded structure is 2.0 nm, according to an NMR structure, and therefore, the compact cylinder is similar in shape to a DNA duplex.[18] Accordingly, in a nanopore experiment at pH 5, the hTelo i-motif yields signals consistent with DNA entry into the vestibule, but neither unfolding nor translocation of the single strand is observed for the captured molecule at 20 °C, even though the melting temperature of the sequence is relatively low, T_m = 47 °C. Addition of a dA_{25} tail still provided no unfolding at pH 5.7, even when the potential was increased to 160 mV. Current reversal was used to discharge the DNA molecule to the same side of the pore from which it entered (Fig. 4).[17]

Raising the pH further to 6.3 or 6.8 introduced an unfolded, single-stranded structure into the population of molecules, and now fast translocations could be observed in addition to long-lived captured species, which we assigned as folded i-motifs.[3] These types of experiments were repeated at several pH values to reveal the dependency of folded lifetime as a function of pH and electrophoretic force. For example, the folding lifetime of the i-motif at physiological pH 7.2 was 9 ms, a value that would be nearly impossible to measure by NMR because only 1% of the strands are folded at that pH.

3. DNA Damage in Telomere Sequences

Our laboratory has a long-standing interest in DNA damage, particularly that derived from oxidative stress or photochemistry.[19,20] Indeed, our original interest in nanopores stemmed from

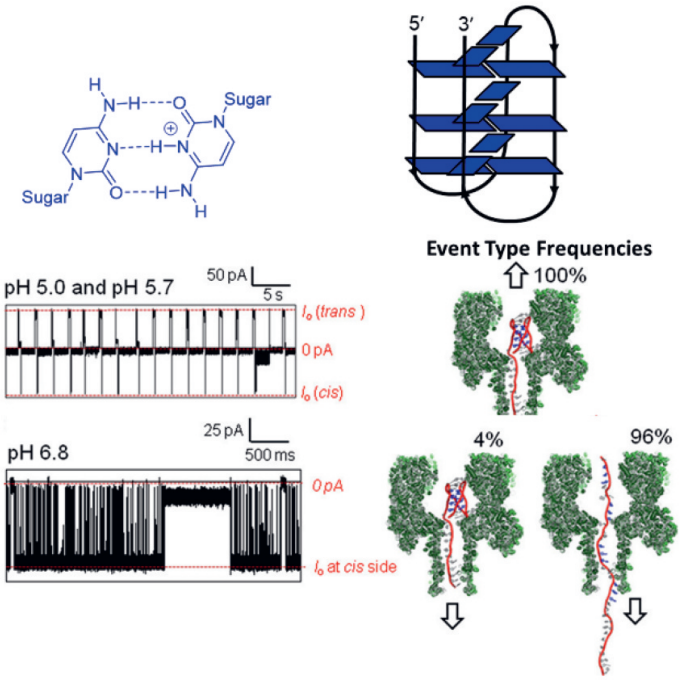

Fig. 4. (Top) The C^+-C base pair and the i-motif fold. (Bottom) The hTelo i-motif produces pH-dependent ionic current patterns when interacting with the α-HL nanopore.

the potential to sequence DNA not just for A, C, G and T, but for modified bases, including lesions, ideally in an experiment that would use native unamplified DNA samples. First, we examined the impact of DNA damage on G-quadruplex folding patterns.

3.1 *Impact of DNA Damage on G4 Folding and Unfolding*

The hTelo repeat sequence contains GGG tracks susceptible to oxidation and TT sequences that form cyclobutane pyrimidine dimers, T=T, when irradiated with UV light.[20,21] The presence of a T=T in a DNA sequence introduces local rotational constraints and slight puckering of the strand.[21] Although it was known that the photodimers could readily form in telomeres, the impact of this lesion within various loops of folded hTelo G4s had not been studied intensively.

We installed T=T lesions synthetically into hTelo G4 sequences in specific locations (Fig. 5).[22] When the T=T was present in the edgewise or diagonal loop of the basket structure, the biophysical data (CD, T_m, *etc.*) were mostly unchanged. In nanopore experiments, the current signatures were analogous to those of G4s without lesions. On the other hand, placing the T=T lesion in a double-chain reversal loop of either the hybrid or propeller forms of the G4 led to unfolding of the G4, releasing one GGG track and forming a triplex. This could be readily detected by the nanopore signature characteristic of an unfolded section that can then dip into the constriction channel, and subsequent further unfolding provides complete translocation. This behaviour was not easily deciphered in any other biophysical experiments, showing the power of the nanopore capture/translocation experiment in providing this model.

Oxidative damage in telomeres leads principally to the oxidized guanine base 8-oxo-7,8-dihydro-guanine, or OG, through the addition of one oxygen atom at C8 and subsequent tautomerization.[20] Such a lesion cannot be well accommodated into the G4 tetrad because Hoogsteen hydrogen bonding requires a lone pair of electrons at N7 of G (Fig. 6). Indeed, synthetic replacement of a G by OG in the core of a G4 lowers the T_m by 15–25 °C.[23] In the hTelo repeat sequence in which the 3' overhang $(GGGTTA)_n$ would have n=10–30, there are abundant opportunities to refold a lesion-containing sequence such that OG would exist in a sin-

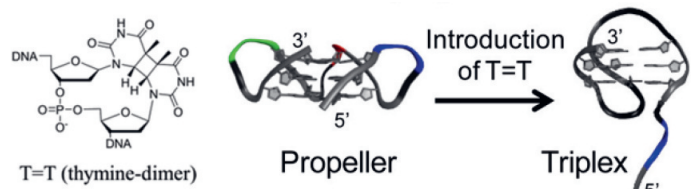

Fig. 5. The presence of a T=T dimer in the hTelo double-chain reversal G4 loop causes unfolding to a triplex structure.

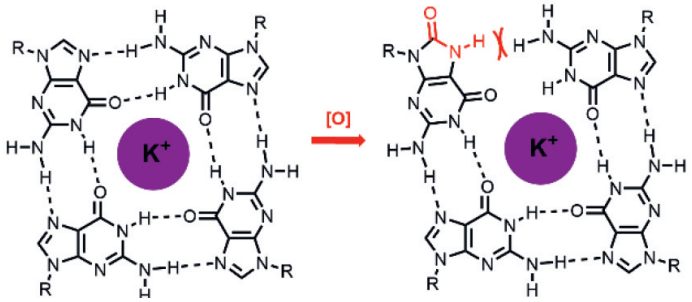

Fig. 6. Oxidation of dG to dOG in a G-tetrad disrupts base pairing and destabilizes the structure.

gle-stranded segment between folded G4s.[24] We first studied the n=5 sequence by replacing the 5'G with OG in either the 1st, 3rd, or 5th GGG track.

Electrical signatures in the nanopore experiment indicated that OG in the 1st or 5th tracks led to normal G4 formation with an unfolded 1st or 5th (OG)GG track. Only the T_m of the 3rd track OG was significantly lower than wild-type sequences by ~ 5 °C, suggestive of a long and somewhat destabilizing central loop being present. In the nanopore experiment, such long-loop G4s probably could not enter the vestibule, accounting for the fact that only triplex-like signatures were observed.

Overall, it appears that lesions can be easily accommodated in the hTelo G4 secondary structure, either by placing the modification into an edgewise loop of the hybrid G4 fold, as with T=T, or by looping out an oxidized G into a loop or single-stranded connecting sequence between adjacent folded G4s (Fig. 7).[22,24]

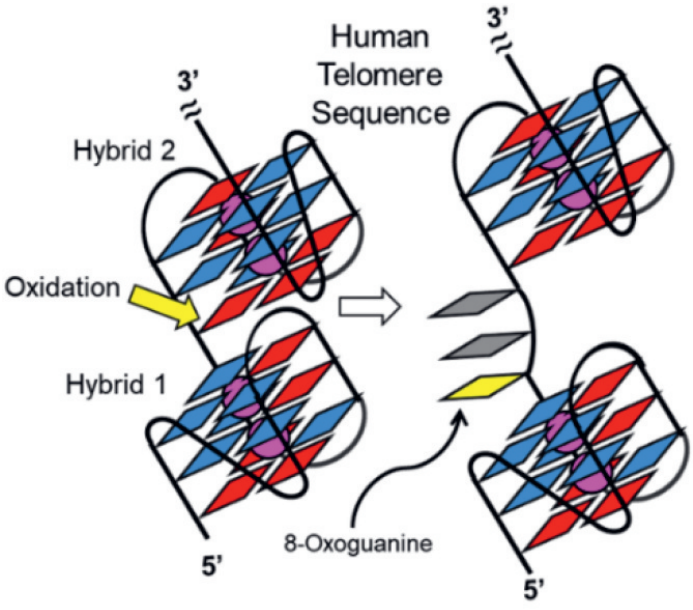

Fig. 7. DNA damage to the core of the human G4 folds disrupts the structure to reside in single-stranded linkers between G4 folds.

3.2 *Detection of 8-oxoguanine in the Human Telomere Repeat Sequence*

Nanopore sequencing at single-nucleotide resolution was still in its infancy in 2015, and a device such as the present ONT MinION was not yet available. One problem with using our Utah α–HL nanopore setup was that translocation of unfolded single-stranded DNA was too fast, ~1 μs per nt, if there was no 'brake' on the oligomer threaded through the nanopore. Nevertheless, we asked the question whether we could use the unfolding process of multiple G4s to slow translocation to look for OG damage sites. The minute change represented by adding one atom to G was certainly going to be too subtle to detect, so we also made specific adducts to OG in order to give a change in the current-blocking signal.

Because OG is easily oxidized, we could use a mild oxidant ($IrBr_6^{2-}$) to induce OG, but not G, oxidation, producing a quinone-like intermediate. In the presence of a nucleophile, in this case a primary amine, an adduct was formed specifically to oxidized OG. The primary amine used was amino-methyl-[18-crown-6], which interacted with the electrolyte (NaCl, KCl, or NH_4Cl) to create a bulky adduct that was stuck in the vestibule for a short time before loss of the cation to collapse the crown ether ring and permit translocation (Fig. 8).

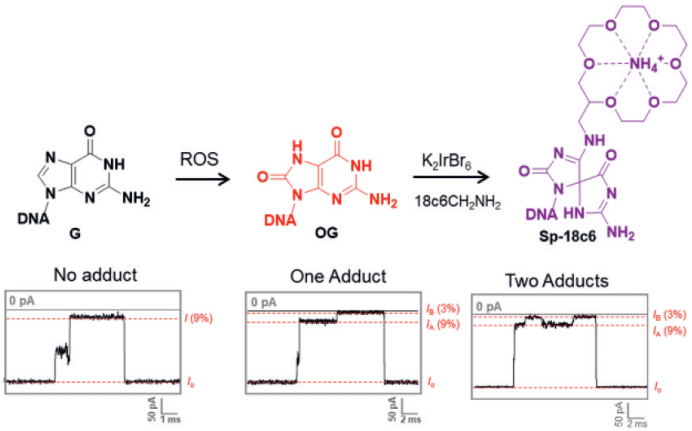

Fig. 8. 18-Crown-6 adducts to dOG in the human telomere permit their detection *via* the α-HL nanopore. The crown ether adduct both slows translocation through the pore and creates a more current-blocking signature.

With everything we learned about nanopore experiments, G4 folding, and OG adduct formation, we were ready to put OG sequencing to the test.[25] In the event, we used 5-$dA_{25}(TTAGGG)_{20}$TT-3' so that only the 5' end of the oligomer would readily thread into the α-HL vestibule. This oligomer was subjected to singlet oxygen oxidation to produce OG at susceptible but unknown sites in the sequence. Using 100 mM NH_4Cl + 2 M LiCl, the repeat sequences folded into the propeller G4s, which can be unravelled at a somewhat consistent speed for entry into the pore.

The quasi-stable crown ether-ammonium complex provided sharp spikes in current blockage that made it easy, in a single-molecule experiment, to count the OG lesions present in each DNA strand. Control experiments indicated that OG sites close together could not be resolved; however, if they were spaced ~30 nucleotides apart, they provided separate signals. Although we had not yet achieved single-nucleotide resolution sequencing, we were able to detect the approximate number and positions of oxidative DNA damage in a 147-mer strand mimicking the hTelo overhang.[25]

4. Progress and Prospects for DNA Damage Sequencing in Human Telomeres

By 2020, single-nucleotide resolution sequencing of DNA amplicons was fast and convenient with the availability of ONT's MinION sequencer. Direct sequencing of RNA and its modifications became possible using 100 ng of RNA extracted from 10^5 cells. DNA modifications pose a significant challenge, however. There are only two copies of each strand per cell, and the overall sequence is much longer. In contrast to RNA epitranscriptomic modifications that are enzymatically written into specific sites in rRNA, tRNA, *etc*., DNA damage modifications occur at very low occupancies and at nearly random sites. Thus, our original dream of sequencing DNA (*e.g.* telomeres) for oxidative damage in a nanopore device is still unrealized. Nevertheless, there has been progress.

First, we examined the wild-type hTelo sequence using an oligomer containing a $d(GGGTTA)_{11}$ insertion and observed a consistent repeat pattern (Fig. 9).

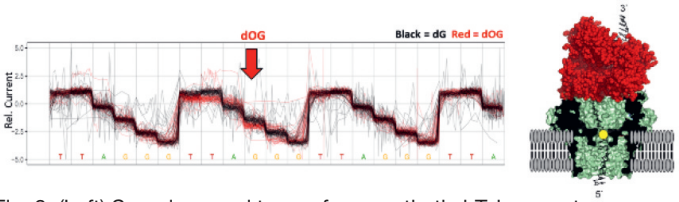

Fig. 9. (Left) Superimposed traces for a synthetic hTelo repeat sequence analysed by ONT sequencing (black) and the same sequence with a single OG replacing the 5' G where marked (red). (Right) Cartoon of the ONT setup.

Next, the synthetic installation of OG at a single 5'-site in one G track (*i.e.* OG-GG) produced a noticeable change in current signature when OG was present at 100% occupancy at that site (Fig. 9; unpublished results). We also studied a plasmid containing a ~900-nt hTelo repeat, and when it was exposed to riboflavin-catalysed photooxidation of G to the extent of about 1% lesion frequency, we were unable to detect any changes in the raw signals from ONT sequencing. Furthermore, in a cellular experiment, OG is most likely to occur at frequencies <0.01% at a given site,[5] and therefore, it is not currently feasible to decipher a single OG event in the noise of the instrument. Further improvements or innovations will be needed.

As a step in this direction, we have developed a method to mark and amplify lesion-containing DNA using an orthogonal third base pair developed by Romesberg and coworkers.[26] Perhaps a combination of enrichment and amplification could eventually lead to successful nanopore sequencing of DNA lesions, and we are actively working toward this goal. We hope that our dream of nanopore sequencing for DNA lesions will become possible. At the present time, the ONT system is an excellent method for sequencing enzymatically installed modifications, either in DNA, *e.g.* 5-methylcytidine, or in RNA, which harbours over one hundred different epitranscriptomic modifications installed usually at high occupancy at specific sites.[27]

Acknowledgements

We are grateful to Prof. H. S. White (University of Utah) for a decade of insight and collaboration, along with the students from both laboratories whose names appear in the references below. The early work with α-HL was funded by a grant from the U.S. National Institutes of Health R01 GM093099; more recently, the application of ONT analysis of DNA/RNA modifications is funded by NIH R35 GM145237.

Author Contributions

C. J. B. wrote the first draft based on discussions with A. F. M., who added edits, figures, and references. Both authors approved the final draft.

[1] A. E. Schibel, N. An, Q. Jin, A. M. Fleming, C. J. Burrows, H. S. White, *J. Am. Chem. Soc*. **2010**, *132*, 17992, https://doi.org/10.1021/ja109501x.
[2] a) L. Song, M. Hobaugh, C. Shustak, S. Cheley, H. Bayley, J. Gouaux, *Science* **1996**, *274*, 1859, https://doi.org/10.1126/science.274.5294.1859; b) D. Stoddart, A. J. Heron, E. Mikhailova, G. Maglia, H. Bayley, *Proc. Natl. Acad. Sci. U. S. A*. **2009**, *106*, 7702, https://doi.org/10.1073/pnas.0901054106; c) J. Kasianowicz, E. Brandin, D. Branton, D. Deamer, *Proc. Natl. Acad. Sci. U. S. A*. **1996**, *93*, 13770, https://doi.org/10.1073/pnas.93.24.13770.
[3] D. Branton, D. W. Deamer, A. Marziali, H. Bayley, S. A. Benner, T. Butler, M. D. Ventra, S. Garaj, A. Hibbs, X. Huang, S. B. Jovanovich, P. S. Krstic, S. Lindsay, X. S. Ling, C. H. Mastrangelo, A. Meller, J. S. Oliver, Y. V. Pershin, J. M. Ramsey, R. Riehn, G. V. Soni, V. Tabard-Cossa, M. Wanunu, M. Wiggin, J. A. Schloss, *Nat. Biotechnol*. **2008**, *26*, 1146, https://doi.org/10.1038/nbt.1495.
[4] Y. Xu, *Chem. Soc. Rev*. **2011**, *40*, 2719, https://doi.org/10.1039/c0cs00134a.
[5] A. M. Fleming, C. J. Burrows, *Nucleic Acids Res*. **2025**, *53*, gkaf1320, https://doi.org/10.1093/nar/gkaf1320.
[6] H. Ren, C. G. Cheyne, A. M. Fleming, C. J. Burrows, H. S. White, *J. Am. Chem. Soc*. **2018**, *140*, 5153, https://doi.org/10.1021/jacs.8b00593.
[7] L. Chen, J. Dickerhoff, S. Sakai, D. Yang, *Acc. Chem. Res*. **2022**, *55*, 2628, https://doi.org/10.1021/acs.accounts.2c00337.
[8] R. D. Gray, J. B. Chaires, *Nucleic Acids Res*. **2008**, *36*, 4191, https://doi.org/10.1093/nar/gkn379.
[9] N. An, A. M. Fleming, E. G. Middleton, C. J. Burrows, *Proc. Natl. Acad. Sci. U. S. A*. **2014**, *111*, 14325, https://doi.org/10.1073/pnas.1415944111.
[10] J. Spiegel, S. M. Cuesta, S. Adhikari, R. Hänsel-Hertsch, D. Tannahill, S. Balasubramanian, *Genome Biol.* **2021**, *22*, 117, https://doi.org/10.1186/s13059-021-02324-z.
[11] P. L. Opresko, S. L. Sanford, M. De Rosa, *Cold Spring Harbor Perspect. Biol*. **2025**, *17*, a041707, https://doi.org/10.1101/cshperspect.a041707.
[12] N. An, A. M. Fleming, C. J. Burrows, *J. Am. Chem. Soc*. **2013**, *135*, 8562, https://doi.org/10.1021/ja400973m.
[13] A. T. Phan, V. Kuryavyi, K. N. Luu, D. J. Patel, *Nucleic Acids Res*. **2007**, *35*, 6517, https://doi.org/10.1093/nar/gkm706.
[14] D. Koirala, T. Mashimo, Y. Sannohe, Z. Yu, H. Mao, H. Sugiyama, *Chem. Commun*. **2012**, *48*, 2006, https://doi.org/10.1039/c2cc16752b.
[15] X. Han, J. L. Leroy, M. Gueron, *J. Mol. Biol*. **1998**, *278*, 949, https://doi.org/10.1006/jmbi.1998.1740.
[16] A. T. Phan, J. L. Mergny, *Nucleic Acids Res*. **2002**, *30*, 4618, https://doi.org/10.1093/nar/gkf597.
[17] Y. Ding, A. M. Fleming, L. He, C. J. Burrows, *J. Am. Chem. Soc*. **2015**, *137*, 9053, https://doi.org/10.1021/jacs.5b03912.
[18] a) A. T. Phan, M. Gueron, J. L. Leroy, *J. Mol. Biol*. **2000**, *299*, 123, https://doi.org/10.1006/jmbi.2000.3613; b) H. R. Drew, R. M. Wing, T. Takano, C. Broka, S. Tanaka, K. Itakura, R. E. Dickerson, *Proc. Natl. Acad. Sci. U. S. A*. **1981**, *78*, 2179, https://doi.org/10.1073/pnas.78.4.2179.
[19] a) W. Luo, J. G. Muller, C. J. Burrows, *Org. Lett*. **2001**, *3*, 2801, https://doi.org/10.1021/ol0161763; b) W. Luo, J. G. Muller, E. M. Rachlin, C. J. Burrows, *Org. Lett*. **2000**, *2*, 613, https://doi.org/10.1021/ol9913643.
[20] A. M. Fleming, C. J. Burrows, *Chem. Res. Toxicol*. **2013**, *26*, 593, https://doi.org/10.1021/tx400028y.
[21] D. G. Su, H. Fang, M. L. Gross, J. S. Taylor, *Proc. Natl. Acad. Sci. U. S. A*. **2009**, *106*, 12861, https://doi.org/10.1073/pnas.0902386106.
[22] A. H. Wolna, A. M. Fleming, C. J. Burrows, *Biochemistry* **2014**, *53*, 7484, https://doi.org/10.1021/bi501072m.
[23] J. Zhou, A. M. Fleming, A. M. Averill, C. J. Burrows, S. S. Wallace, *Nucleic Acids Res*. **2015**, *43*, 4039, https://doi.org/10.1093/nar/gkv252.
[24] N. An, A. M. Fleming, C. J. Burrows, *ACS Chem. Biol.* **2016**, *11*, 500, https://doi.org/10.1021/acschembio.5b00844.
[25] N. An, A. M. Fleming, H. S. White, C. J. Burrows, *ACS Nano* **2015**, *9*, 4296, https://doi.org/10.1021/acsnano.5b00722.
[26] a) J. Riedl, Y. Ding, A. M. Fleming, C. J. Burrows, *Nat. Commun*. **2015**, *6*, 8807, https://doi.org/10.1038/ncomms9807; b) D. A. Malyshev, Y. J. Seo, P. Ordoukhanian, F. E. Romesberg, *J. Am. Chem. Soc*. **2009**, *131*, 14620, https://doi.org/10.1021/ja906186f.
[27] A. M. Fleming, C. J. Burrows, *RNA* **2026**, ASAP, https://doi.org/10.1261/rna.080908.125.

The definitive version of this article is the electronic one that can be found at https://doi.org/10.2533/chimia.2026.120

Received: January 15, 2026